

Phospholipid-Coated Gas Bubble Engineering: Key Parameters for Size and Stability Control, as Determined by an Acoustical Method

Simona Rossi, Gilles Waton, and Marie Pierre Krafft*

Systèmes Organisés Fluorés à Finalités Thérapeutiques (SOFFT), Université de Strasbourg, Institut Charles Sadron (CNRS), 23 rue du Loess, 67034 Strasbourg Cedex 2, France

Received July 16, 2009. Revised Manuscript Received August 26, 2009

We have recently reported the sampling of differently sized monomodal populations of microbubbles from a polydisperse lipid-coated bubble preparation. The microbubbles were coated with dimyristoylphosphatidylcholine (DMPC) and stabilized by perfluorohexane (PFH). Such microbubbles are useful as contrast agents and, potentially, for oxygen, drug, and gene delivery and as therapeutic devices. Monomodal populations of small bubbles ($\sim 1.6 \mu\text{m}$ in radius) and large bubbles ($\sim 5.4 \mu\text{m}$) have been obtained, as assessed by acoustical measurement, static light scattering, and optical microscopy. In this paper, we have determined the influence of various preparation parameters on the initial size characteristics (mean radius and radii distribution) of the microbubbles and on their stability upon time. The bubble size was determined acoustically, with a homemade acoustic setup equipped with a low-power emitter, to avoid altering the bubble stability. We have focused on the effects of the bubble flotation time during the fractionation process and on the DMPC concentration. PFH was indispensable for obtaining stable bubbles. The nature of the buffer [Isoton II vs *N*-2-hydroxyethylpiperazine-*N'*-2-ethanesulfonic acid (HEPES)] used as the continuous phase did not significantly impact the bubble characteristics and stability. In both buffers, the half-lives of small bubbles ($\sim 1.6 \mu\text{m}$ in radius in Isoton II and $\sim 2.1 \mu\text{m}$ in HEPES) were found to be longer than those of larger ones (~ 5.4 and $\sim 5.9 \mu\text{m}$ in Isoton II and HEPES, respectively). The bubble stability study revealed that in both buffers, the average radius of the population of large bubbles progressively increased with time. On the other hand, the average radius of the population of small bubbles decreased slightly in Isoton II and remained constant in HEPES. This suggests that the dissolution behavior of small and large bubbles is governed by different mechanisms.

Introduction

Microbubbles have considerable potential in diagnostics and therapy. The first generation of bubble-based contrast agents for diagnostic ultrasound imaging is commercially available.^{1–4} Intravascular transport of oxygen in the form of stabilized micrometer-sized bubbles is, in principle, a simple and cost-effective means of delivering oxygen to tissues.^{5,6} Further applications under investigation include targeted microbubbles for molecular imaging,^{3,7} ultrasound-triggered drug and gene delivery, and use as clot-breaking agents.^{4,8,9}

A major limitation in the development of microbubbles for intravascular use was that air (or oxygen or nitrogen) bubbles dissolve rapidly in the blood under the combined action of Laplace pressure and arterial blood pressure. Perfluorocarbons (PFCs), when used as part of the bubble-filling gas, retard bubble dissolution effectively, due to very low water solubility, allowing the half-life of the bubbles to increase from a few seconds to several minutes.¹ Because of their high biological inertness, high oxygen solubility, and extremely low solubility in water, PFCs are

being investigated for a range of biomedical uses, including intravascular oxygen transport,⁶ ophthalmology,¹⁰ drug delivery, diagnosis, and biomedical research.^{11,12} Their biocompatibility and pharmacodynamics are therefore well-documented.^{6,13}

Besides the PFC approach to stabilization, proper shell engineering and preparation conditions can help stabilize microbubbles against both dissolution and coalescence. Various hard shells made of biodegradable block copolymers, such as poly(D,L-lactide-co-glycolide)¹⁴ or polyelectrolyte multilayers,¹⁵ have been investigated. However, soft bubble shells are usually deemed preferable for contrast agent applications as they only minimally dampen sound wave oscillations. Soft shells are also considered advantageous for traversing capillary beds.¹ Molecular surfactants or combinations of surfactants that enhance stability by decreasing the interfacial tension and, hence, the Laplace pressure have therefore been investigated. It has been demonstrated that, in the absence of a PFC gas, the stability of air-filled phospholipid-coated microbubbles was primarily related to the resistance of the lipid monolayer shell to gas permeation.¹⁶ It was shown that oxygen permeability through condensed phospholipid monolayers

*To whom correspondence should be addressed. Fax: (+33)3 88 41 40 99. E-mail: krafft@ics.u-strasbg.fr.

(1) Schutt, E. G.; Klein, D. H.; Mattrey, R. M.; Riess, J. G. *Angew. Chem., Int. Ed.* **2003**, *42*, 3218–3235.

(2) Feinstein, S. B. *Am. J. Physiol. Heart Circ. Physiol.* **2004**, *287*, H450–H457.

(3) Lindner, J. R. *Nat. Rev. Drug Discovery* **2004**, *3*, 527–532.

(4) Unger, E. C.; Porter, T.; Culp, W.; Labell, R.; Matsunaga, T.; Zutshi, R. *Adv. Drug Delivery Rev.* **2004**, *56*, 1291–1314.

(5) van Liew, H.; Burkard, M. *Adv. Exp. Med. Biol.* **1997**, *411*, 395–401.

(6) Riess, J. G. *Chem. Rev.* **2001**, *101*, 2797–2920.

(7) Kaufmann, B. A.; Lindner, J. R. *Curr. Opin. Biotechnol.* **2007**, *18*, 11–16.

(8) Ferrara, K.; Pollard, R.; Borden, M. *Annu. Rev. Biomed. Eng.* **2007**, *9*, 415–447.

(9) Hernot, S.; Klibanov, A. L. *Adv. Drug Delivery Rev.* **2008**, *60*, 1153–1166.

(10) Rico-Lattes, I. In *Fluorine and Health. Molecular Imaging, Biomedical Materials and Pharmaceuticals. Advances in Fluorine Science*; Tressaud, A., Haufe, G., Eds.; Elsevier: Amsterdam, The Netherlands, 2008; p 407.

(11) Krafft, M. P. *Adv. Drug. Delivery Rev.* **2001**, *47*, 209–228.

(12) Krafft, M. P.; Riess, J. G. *J. Polym. Sci. Part A: Polym. Chem.* **2007**, *45*, 1185–1198.

(13) Flaim, S. F. *Artif. Cells, Blood Substitutes, Immob. Biotechnol.* **1994**, *22*, 1043–1054.

(14) Forsberg, F.; Lathia, J. D.; Merton, D. A.; Liu, J.-B.; Le, N. T.; Goldberg, B. B.; Wheatley, M. A. *Ultrasound Med. Biol.* **2004**, *30*, 1281–1287.

(15) Shchukin, D. G.; Köhler, K.; Möhwald, H.; Sukhorukov, G. B. *Angew. Chem., Int. Ed.* **2005**, *44*, 3310–3314.

(16) Pu, G.; Longo, M. L.; Borden, M. A. *J. Am. Chem. Soc.* **2005**, *127*, 6524–6525.

decreases exponentially with increasing lipid acyl chain length. However, the in vivo half-life of 7–8 μm -sized bubbles stabilized by dipalmitoylphosphatidylcholine (DPPC) does not exceed a few minutes.¹

A difficulty that hampers the investigation of soft microbubbles is that the methods that allow preparation of samples large enough for physicochemical and biomedical experimentation, that is, mechanical agitation or sonication, generally yield highly polydisperse samples. Although significant progress has been achieved using the coaxial electrohydrodynamic atomization (CEDHA) method^{17,18} and techniques based on microfluidic devices,^{17–21} their output does not yet appear satisfactory. In addition, certain applications such as oxygen or drug delivery require bubbles smaller than 5 μm . Bubbles between 2 and 8 μm in diameter have been obtained by CEDHA.²² The production of small bubbles with microfluidics would require very fine channels (~ 7 μm diameter) and higher gas flow rates, which would augment polydispersity.^{17,18} It is noteworthy, however, that monodisperse microbubbles down to 2 μm have recently been obtained with microfluidics.^{21,23}

Mechanical agitation and sonication remain methods of choice for the rapid production of large amounts of microbubbles but with high polydispersity. Much less polydisperse populations of bubbles can be obtained from these preparations by fractionation using flotation. A good correlation has previously been found between measured size values and those predicted by a dynamic model developed for the size fractionation by flotation of microbubbles having a heat-denatured human albumin shell.²⁴ A fraction of submicrometric microbubbles (~ 0.45 μm), with a shell made of Span and Tween surfactants, has been separated by centrifugation or gravity from a larger mean-sized sonicated preparation.²⁵ Recently, we have shown that a polydisperse preparation of dimyristoylphosphatidylcholine (DMPC)-coated microbubbles stabilized by perfluorohexane (PFH) and produced by sonication could be fractionated, simply under the action of gravity, into narrowly dispersed subpopulations of different sizes.²⁶ Samples of bubbles with sizes narrowly dispersed around mean radii of 1.6 and 5.4 μm have thus been isolated. Centrifugal fractionation of microbubbles coated with distearoylphosphatidylcholine (DSPC) and stabilized by perfluorobutane (PFB) has also been reported.²⁷

Another difficulty encountered in the investigation of soft bubbles concerns the measurement of their initial size and of their stability over time. The most important limitations of the commonly used sizing methods such as the electrical zone sensing (EVS) method, the single-particle optical sensing (SPOS) method, and the static (also called laser diffraction) or dynamic (also called photon correlation spectroscopy) light scattering methods are

that the bubbles tend to float due to their buoyancy and that the sample is modified during the measuring process, which prevents monitoring of the stability of a given bubble sample upon time. Acoustical methods based on the measurement of the attenuation coefficient of an ultrasound wave that propagates in a dispersion of bubbles have been developed.^{28–32} These methods present definite advantages over the nonacoustical sizing methods. First, the measurement is independent of bubble movement. Therefore, the sample can be stirred effectively to avoid bubble floating and aggregation. The measurement is performed on the whole population and is rapid (less than 0.5 s), allowing bubble stability studies. We have recently developed a multifrequency acoustical setup to determine the size of microbubbles.²⁶ The mean sizes and size distributions, as measured by this method, have been confirmed by static light diffraction and optical microscopy.²⁶ The major assets of our technique are a low-power acoustical signal, which avoids alteration of bubble stability, and a good precision on the absorption coefficient determination (see the Materials and Methods). The device is fully automated, with the possibility of collecting many hundreds of data points over long periods (e.g., 8 h).

The present article takes advantage of the possibility of producing samples with differently sized microbubbles and of the acoustic bubble sizing device to investigate the effects of formulation and preparation conditions on the size and stability characteristics of microbubbles coated by DMPC and stabilized by PFH. Such information is all the more important that bubbles constitute an out-of-equilibrium system; bubble size characteristics are, therefore, highly sensitive to the preparation methodology. The preparation protocol utilized includes hydration of DMPC in an aqueous buffer solution, formation of a foam by sonication of a dispersion of hydrated phospholipid under an atmosphere of nitrogen saturated with PFH, and dilution of this foam with the same buffer, which leads to individualized microbubbles in suspension in an aqueous phase. The time during which the bubbles are allowed to float in the preparation medium after their individualization and prior to use (e.g., injection in the ultrasound measuring cell) was highly critical and allowed sorting of the bubbles according to size. The effects of the concentration of the wall-forming component (DMPC) and of the presence or absence of PFH in the bubble filling gas (N_2) were also investigated. Finally, the influence of the nature of the buffered aqueous phase in which the initial foam is diluted to produce the individual bubbles has been examined.

Materials and Methods

Materials. 1,2-Dimyristoyl-*sn*-glycero-3-phosphatidylcholine (DMPC) was purchased as a dry powder from Avanti Polar Lipids (Alabaster, AL) and used as received. PFH (C_6F_{14} ; purity, > 99%) and Pluronic F68 (a polyoxyethylene–polyoxypropylene triblock copolymer; MW ~ 8300 ; purity, > 99%) were from Sigma. The Isoton II diluent was obtained from Coulter Beckman (pH 7.4; Miami, FL). A solution of HEPES (*N*-2-hydroxyethyl-piperazine-*N'*-2-ethanesulfonic acid, Sigma) (20 mM) in 150 mM NaCl was prepared, and its pH was adjusted to 7.4 with 0.1 N NaOH. Water was purified using a Millipore system (pH 5.5; surface tension, 72.1 mN m^{-1} at 20 °C; resistivity, 18 M Ω cm).

(28) De Jong, N.; Hoff, L.; Skotland, T.; Bom, N. *Ultrasonics* **1992**, *30*, 95–103.

(29) Frinking, P. J. A.; De Jong, N. *Ultrasound Med. Biol.* **1998**, *24*, 523–533.

(30) Goertz, D. E.; de Jong, N.; van der Steen, A. F. W. *Ultrasound Med. Biol.* **2007**, *33*, 1376–1388.

(31) Sarkar, K.; Shi, W. T.; Chatterjee, D.; Forsberg, F. J. *Acoust. Soc. Am.* **2005**, *118*, 539–550.

(32) Tang, M.-X.; Eckersley, R. J.; Noble, J. A. *Ultrasound Med. Biol.* **2005**, *31*, 377–384.

(17) Stride, E.; Edirisinghe, M. J. *Med. Biol. Eng. Comput.* **2009**, *47*, 883–893.

(18) Stride, E.; Edirisinghe, M. J. *Soft Matter* **2008**, *4*, 2350–2359.

(19) Xu, J. H.; Li, S. W.; Wang, Y. J.; Luo, G. S. *Appl. Phys. Lett.* **2006**, *88*, 133506-1–133506-3.

(20) Pancholi, K. P.; Farook, U.; Moaleji, R.; Stride, E.; Edirisinghe, M. J. *Eur. Biophys. J.* **2008**, *37*, 515–520.

(21) Talu, E.; Hettiarachchi, K.; Powell, R. L.; Lee, A. P.; Dayton, P. A.; Longo, M. L. *Langmuir* **2008**, *24*, 1745–1749.

(22) Farook, U.; Stride, E.; Edirisinghe, M. J.; Moaleji, R. *Med. Biol. Eng. Comput.* **2007**, *45*, 781–789.

(23) Talu, E.; Hettiarachchi, K.; Zhao, S.; Powell, R. L.; Lee, A. P.; Longo, M. L.; Dayton, P. A. *Mol. Imaging* **2007**, *6*, 384–392.

(24) Kvåle, S.; Jacobsen, H. A.; Asbjørnsen, O. A.; Omtveit, T. *Sep. Technol.* **1996**, *6*, 219–226.

(25) Wheatley, M. A.; Forsberg, F.; Dube, N.; Patel, M.; Oeffinger, B. E. *Ultrasound Med. Biol.* **2006**, *32*, 83–93.

(26) Rossi, S.; Waton, G.; Krafft, M. P. *ChemPhysChem* **2008**, *9*, 1982–1985.

(27) Feshitan, J. A.; Chen, C. C.; Kwan, J. J.; Borden, M. A. *J. Colloid Interface Sci.* **2009**, *329*, 316–324.

Preparation of the Bubble Dispersions. DMPC (10, 24, 50, or 100 mmol L⁻¹) was dispersed by magnetic stirring in the buffer solution, Isoton II or HEPES, depending on the experiment, for 3–6 h at room temperature. Pluronic F68 was added to facilitate phospholipid dispersion and foam formation (DMPC:F68 molar ratio 10:1). A 1 mL aliquot of the DMPC/F68 dispersion was transferred to a glass tube (2 cm in diameter) and presonicated under air at low power (setting 3, duty cycle 40%) for 30 s at 25 °C. The sonicator (Vibracell sonicator, Bioblock Scientific, Illkirch, France) was equipped with a 3 mm titanium probe and operated at 20 kHz. The dispersion was then sonicated for 15 s (setting 5, duty cycle 40%) at 25 °C under nitrogen or under a N₂ atmosphere saturated with PFH. In the latter case, N₂ was allowed to bubble through three vials containing PFH (a liquid at room temperature) before being flushed into the glass tube. The probe was consistently placed 5 mm below the surface of the dispersion. The resulting aggregated microbubble suspension (foam) was immediately diluted with 14 mL of the buffer (Isoton II or HEPES). Bubbles were allowed to float for different times (3, 5, 10, and 20 min), depending on the experiment, and aliquots were injected in the ultrasonic cell that was filled with the buffer used for the preparation (cell volume, 140 mL). To keep the initial values of the attenuation coefficient comparable, the injected volumes of bubble dispersions ranged from 300 μL to 1 mL, depending on bubble sizes (i.e., after flotation times of 3, 5, 10, and 20 min).

Acoustical Determination of Microbubble Size Distribution. The method that we have set up to determine the size of microbubbles is based on the reduction in amplitude (attenuation coefficient) of an acoustical pulse that propagates through the aqueous bubble dispersion. A procedure has been developed that fits standard simple-harmonic resonator curves to measured attenuations to infer the size of the bubbles, according to a known procedure.^{28,30,33,34}

When a bubble is mechanically excited by a pressure impulse or an acoustical wave, it oscillates. A simple analogy for this consists of a mass attached to a spring. The spring that provides the restoring force models the gas in the bubble. The inertia effect is dominated by the motion of the liquid surrounding the bubble. Thus, a bubble is an oscillator whose resonance frequency, f_0 , is given by eq 1.³⁴

$$f_0^2 = \frac{1}{4\pi^2 \rho R_0^2} \left[3\kappa \left(p_0 + \frac{2\sigma}{R_0} \right) - \frac{2\sigma}{R_0} \right] \quad (1)$$

where R_0 is the radius of the bubble, ρ is the density of the continuous phase, κ is the polytropic index, p_0 is the atmospheric pressure, and σ is the interfacial tension (i.e., 42 mN m⁻¹ for DMPC at the air/water interface, as assessed by tensiometry).

This simple model is valid in our case because the shell of the bubbles is made of DMPC, which forms a fluid film with very low viscosity. The nonlinear effects are ignored because the acoustical power is very low (<0.1 W cm⁻²). Multiple diffraction is also ignored because the concentration of bubbles is sufficiently low in our experiments ($\sim 2 \times 10^7$ bubbles in the acoustical cell). By contrast with the soft DMPC shell, the hard shells of most contrast agents have required the development of more complex models.^{31,35–37}

The oscillation of the bubble is dampened by viscous loss, acoustical emission, and thermal exchange between the bubble and the surrounding medium. When ultrasonic waves propagate through a bubble-containing medium, the coupling between bubble and acoustic field induces absorption and dispersion of the acoustic wave. For a low-amplitude plane wave and a low

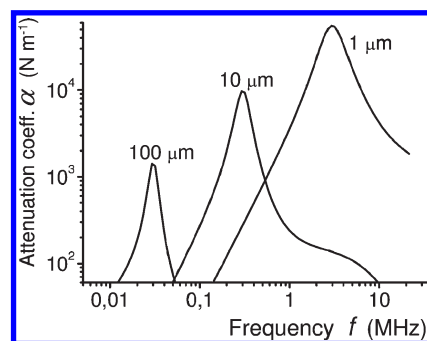


Figure 1. Variation of the attenuation coefficient of an ultrasound wave that propagates in a monodisperse aqueous dispersion of microbubbles (100, 10, or 1 μm), as a function of frequency. The bubble concentration is 0.1% v/v.

bubble concentration, the attenuation coefficient, α , is given by eq 2:³⁴

$$\alpha = \frac{f^2}{2\pi k} \frac{3X_b}{R_0^2} \frac{\beta f}{(f_0^2 - f^2)^2 + 4(\beta f)^2} \quad (2)$$

where f is the frequency, k is the wavenumber of the acoustic wave ($k = 2\pi f/c$), X_b is the volume fraction of bubbles, and β is the sum of viscous, diffraction, and thermal effects; β is given by eq 3,

$$\beta = \frac{2\mu}{\rho R_0^2} + \frac{R_0(2\pi f)^2}{2c} + 3 \frac{p_g}{4\pi \rho f R_0^2} \text{Im}(\kappa) \quad (3)$$

where c is the velocity of sound and μ is the viscosity of the surrounding medium.

The attenuation coefficient has been calculated as a function of frequency using eqs 2 and 3 (Figure 1). The attenuation is maximal when the frequency of the acoustic wave is equal to the resonance frequency of the bubble.

The bubble radius can be determined using eq 2. For a polydisperse distribution of sizes, the wave attenuation spectrum is given by:

$$\alpha(f) = \int_{R_1}^{R_2} \frac{\omega^2}{k} \frac{3X_b(R)}{R^2} \frac{\beta(R, \omega)}{(\omega_0^2 - \omega^2)^2 + 4[\beta(R, \omega)]^2} dR \quad (4)$$

where $\omega = 2\pi f$ is the angular frequency.

The size distribution was obtained by minimizing the square errors between the experimental values and the values obtained from eq 4. The continuous size distribution was built up by: (i) attributing a value to the fitting parameters $X_b(R_i)$ (i.e., the bubble volume fractions at a given radius) for 10–15 chosen radius values and (ii) interpolating these fitting parameters with a spline line. Optimization of the continuous size distribution was then achieved using an iteration process.

Ultrasound Transmission Setup. The attenuation spectra were measured using a homemade ultrasonic pulse setup. The frequency range was chosen as 0.3–6.6 MHz, which corresponds to resonance frequencies of bubbles whose sizes are between ~ 0.4 and $\sim 10 \mu\text{m}$. The cubic cell, schematically represented in Figure 2, was built using two glass walls (BK-7, standard optical polish, 4 cm thick, Schott, Clichy France) separated by two glass plates (BK-7, 1.5 cm thick) a distance of 4 cm.

The two lateral glass walls were metallized using a thin layer of silver varnish. Two circular piezoelectric transducers (PZT; 1 mm thick; 2.5 cm in diameter; resonance frequency, ~ 2.2 MHz; Polytech, Pantin, France) were set on the glass walls of the cell, the acoustical contacts being achieved using a thin layer of mineral oil. The emitter and receiver transducers were enclosed in a piece of brass and connected to the generator or the receptor, respectively.

(33) Medwin, H. J. *Acoust. Soc. Am.* **1977**, *62*, 1041–1044.

(34) Leighton, T. G. *The Acoustic Bubble*; Academic Press: San Diego, 1994.

(35) Church, C. C. J. *Acoust. Soc. Am.* **1995**, *97*, 1510–1521.

(36) Takeuchi, S.; Sato, T.; Kawashima, N. *Colloids Surf., B* **2002**, *24*, 207–216.

(37) Doinikov, A. A.; Dayton, P. A. J. *Acoust. Soc. Am.* **2006**, *120*, 661–669.

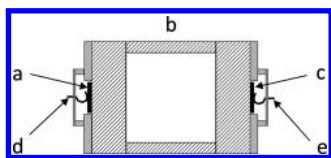


Figure 2. Multifrequency acoustical setting used for the investigation of microbubbles. The emitting transducer (a) is excited with seven narrowband wave packages (0.45, 0.75, 1.2, 2.4, 3.3, 5.7, and 6.6 MHz). The ultrasound signal goes through a glass cell (140 mL, b) containing the test material and is received by a second transducer (c) that converts it into an electrical signal. The emitter and receiver transducers are enclosed in a piece of brass and connected to the generator (d) or the receptor (e), respectively.

The emitting signal was produced by an arbitrary waveform generator (MI 6030, Spectrum, GrossHansDorf, Germany). The received signal was preamplified (40 dB gain, Sofranel, Sartrouville, France) and recorded on a PC computer with a converter board (MI 3025, Spectrum). To obtain a large frequency range (0.3–8 MHz), seven successive short ($\sim 10 \mu\text{s}$) wave pulses were emitted at central frequencies of 0.45, 0.75, 1.2, 2.4, 3.3, 5.7, and 6.6 MHz. The main advantage of processing numerous narrowband signals is that, because of a better signal/noise ratio, a higher precision of the Fourier transform of the signal is obtained, as compared to processing a smaller number of broadband signals.

The setup has been designed so that the ultrasound field does not alter the stability of the bubbles: First, the acoustical power that we used is low ($< 0.1 \text{ W cm}^{-2}$; peak-to-peak acoustical pressure, $< 3 \times 10^4 \text{ Pa}$). Second, the wave package only lasts $10 \mu\text{s}$, and only 256 data points were recorded during the whole experimental span time along a pseudologarithmic scale, ensuring that the bubbles were only weakly exposed to ultrasound. We checked that there was no difference in bubble dissolution rate when the wave package was emitted at different time intervals (from $\sim 15 \text{ s}$ to 1 min). The ultrasound emission time was actually less than 30 ms. However, because the acoustical path comprises four interfaces (emitter/glass, glass/water, water/glass, and glass/receiver), the signal at the receiver transducer presents several peaks due to the multiple reflections of the ultrasound wave in the cell. This may induce a slightly longer time exposure of the microbubbles to the ultrasound.

Only the first peak of the transmitted signal, which corresponds to the shortest path of the acoustical wave, was taken into account in the signal treatment. A fast Fourier transform (FFT) of this signal was worked out. A discrete spectrum with steps of 100 kHz was obtained for each emitted pulse. Only the values in the neighborhood of the maximum of the FFT were taken into account. These values were divided by the values obtained in the absence of bubbles.

It is noteworthy that no data can be obtained for the frequency value of $\sim 4.4 \text{ MHz}$, which corresponds to the second harmonic of the transducer. The precision on the absorption coefficient is $\sim 0.03 \text{ N cm}^{-1}$. This error originates from the stirring used to prevent creaming of the bubbles. When the stirrer is stopped, the precision is better than 0.005 N cm^{-1} .

The microbubbles were maintained under stirring ($\sim 250 \text{ rpm}$) during measurements and thermoregulated at $25^\circ \pm 1^\circ \text{C}$. It was checked that the aqueous phase was saturated with the diffusing bubble gases. All experiments were performed in triplicate. We checked by differential scanning calorimetry that DMPC was in its fluid phase state in both buffer solutions utilized. All distributions are given in volume, and polydispersity is expressed in terms of width at half height.

Optical Microscopy. The samples were observed by optical microscopy (Olympus BH2, Tokyo, Japan). Three to four droplets of bubble sample were placed into a concave slide and covered with a glass slide. Rapid image acquisition was achieved using a Lumenera Infinity 2 CCD camera (Lumenera, Ottawa,

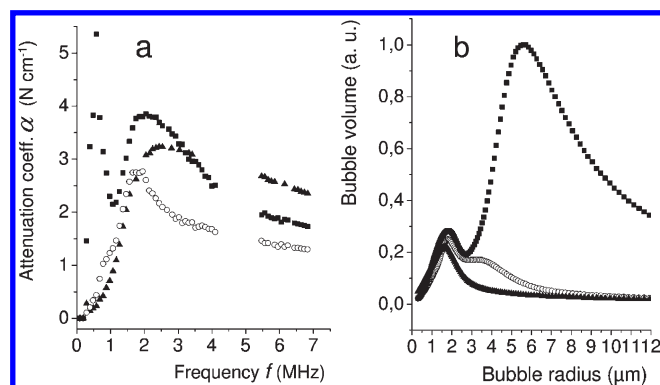


Figure 3. (a) Variation of the attenuation coefficient, α , as a function of the ultrasound frequency, f , for microbubbles prepared from 50 mM concentrated DMPC dispersions injected after flotation for 3 (squares), 10 (circles), and 20 min (triangles). (b) Bubble radius distributions (same symbols as for the flotation times), as determined from the ultrasound absorption spectra plotted in panel a.

Canada). Bubble radii were measured using the ImageJ software package.³⁸

Results and Discussion

Parameters That Influence the Initial Size of Bubbles.

Flotation Time. Under the action of gravity, microbubbles tend to migrate to the air/water interface at a rate that depends on their size. We took advantage of this property to sort out bubbles into monomodal populations. Bubbles were therefore harvested after 3, 5, 10, or 20 min of flotation by pipeting them consistently at the same level in the preparation tube. The variously sized populations were then injected in the ultrasound cell, and the variation of the attenuation coefficient α was measured as a function of time for a range of ultrasound frequencies f . Figure 3a shows the variation of α as a function of f at the initial time t_0 , that is, 107 s after injection in the ultrasound cell for PFH-saturated N_2 bubbles obtained from a 50 mM-concentrated DMPC dispersion.

The bubble size distributions (in volumes) were determined from the ultrasound absorption spectra. Figure 3b shows that after 3 min of flotation, a bimodal size distribution was obtained with a dominant ($\sim 90\%$) population of large bubbles centered around $\sim 5.4 \mu\text{m}$ coexisting with a smaller ($\sim 10\%$) population of bubbles at $\sim 1.6 \mu\text{m}$. Increasing the flotation time to 5 min (not shown) shifted the main bubble population to about $4 \mu\text{m}$, partly overlapping the population of small bubbles at $1.6 \mu\text{m}$. When the flotation time was increased to 10 min, the main population was found at smaller radii ($1.8\text{--}2 \mu\text{m}$). A shoulder revealed the presence of some remaining larger bubbles ($3.2\text{--}4 \mu\text{m}$). After 20 min of flotation, the bubble size distribution was primarily characterized by a monomodal population centered at $\sim 1.6 \mu\text{m}$. Thus, increasing the flotation time from 3 to 20 min allowed sorting out of bubbles of different sizes. Essentially, monomodal populations of bubbles with a distinct average radius and low polydispersity (standard deviation, SD) could be produced ($\sim 1.6 \pm 0.4$ and $\sim 5.4 \pm 0.3 \mu\text{m}$).

DMPC Concentration. The effect of four DMPC concentrations (10, 24, 50, and 100 mM) on the bubble's initial size characteristics was studied for two flotation times, 3 and 20 min. Figure 4 shows the variation of α as a function of f in these studies.

Figure 5 shows the distributions in volume as determined from the attenuation spectra. After 3 min of flotation, the 10 mM

(38) Rasband, W. S. *ImageJ*; U.S. National Institute of Health: Bethesda, MD, 1997–2005; <http://rsb.info.nih.gov/ij/>.

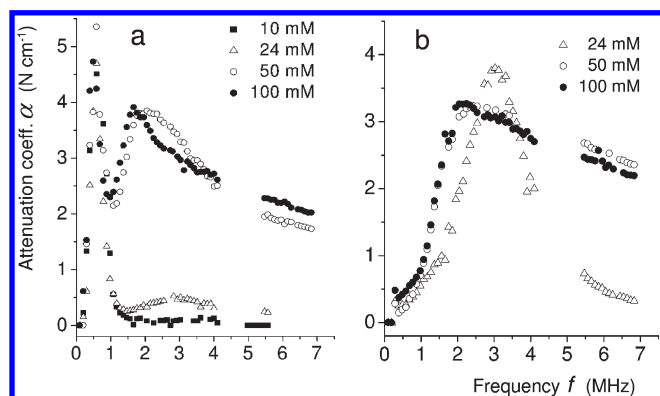


Figure 4. Variation of the attenuation coefficient, α , as a function of ultrasound frequency, f , for microbubbles prepared from variously concentrated DMPC dispersions (10, 24, 50, and 100 mM) and collected after (a) 3 and (b) 20 min of flotation.

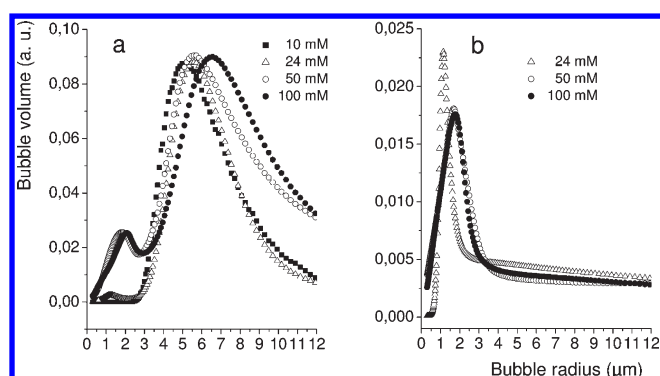


Figure 5. Radii distributions for bubbles prepared from 10, 24, 50, and 100 mM-concentrated DMPC dispersions and injected after (a) 3 and (b) 20 min of flotation, as calculated from the corresponding attenuation spectra featured in Figure 4a,b.

DMPC dispersions led to monomodal populations of bubbles ($\sim 5.4 \pm 0.3 \mu\text{m}$ in radius, Figure 5a). Under the same conditions, the 24, 50, and 100 mM dispersions led to bimodal populations, centered at ~ 5.5 – 6.5 (dominant, $\sim 90\%$ or more) and $\sim 2 \mu\text{m}$ ($\sim 10\%$ or less), respectively. This indicates that ~ 24 mM is a critical DMPC concentration value to form “small” bubbles, $\sim 2 \mu\text{m}$ in radius.

Increasing the flotation time to 20 min led to monomodal bubble populations for all of the concentrations investigated, except for the lowest one (10 mM), for which no bubble remained present. The 50 and 100 mM-concentrated dispersions led to a mean bubble radius of $1.6 \pm 0.4 \mu\text{m}$, while the 24 mM dispersions led to a significantly lower mean radius of $\sim 1.0 \mu\text{m}$ and a lower polydispersity ($\pm 0.2 \mu\text{m}$); however, the number of small bubbles obtained in the latter case was three times smaller.

It can be seen that the peak position of the bubble size distribution increases, as well as the polydispersity, with the DMPC concentration, irrespective of the flotation time. This may indicate that an excess of DMPC favors rapid coalescence of the large bubbles, as was shown for emulsions.³⁹

These data show that the DMPC concentration has an important impact on the bubble formation process, in particular when obtaining small, narrowly dispersed bubbles is sought after. One reason for this is that for a given volume of bubbles, the

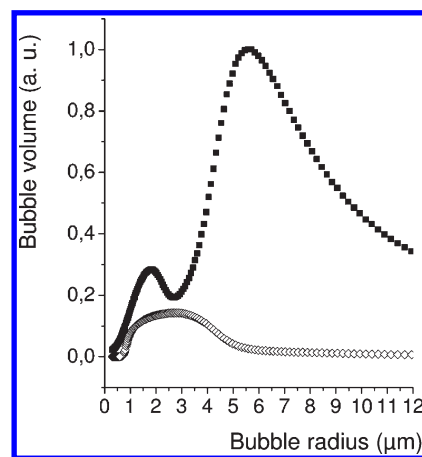


Figure 6. Size distributions of microbubbles obtained from a 50 mM DMPC dispersion after 3 min of flotation. The filling gas was N_2 (empty rhombs) or N_2 saturated with PFH (full squares). The volume injected in the ultrasonic cell was $300 \mu\text{L}$.

smaller their size, the more DMPC molecules are needed, since, at constant volume, the bubble surface increases as $R^{3/2}$.

Presence of PFH. Ultrasound attenuation measurements were carried out with bubbles formed from 50 mM DMPC dispersions in the presence or absence of a PFC gas. The PFC chosen was PFH, because it is even less water-soluble than those (perfluoropentane or PFB) that are being used to retard bubble dissolution for practical diagnostic ultrasound examination and should therefore procure longer bubble life times.^{1,40} The bubbles were analyzed after 3 min of flotation time. The results are shown in Figure 6.

It can be seen that the overall bubble volume fraction was significantly lower when PFH was absent. Only a broad population centered $\sim 2.5 \pm 0.6 \mu\text{m}$ was observed. The population centered at $5.6 \mu\text{m}$, which was largely predominant when PFH was present, had not formed, or had already disappeared.

Buffer: Isoton vs HEPES. Figure 7 shows the initial size distributions of 10 and 50 mM DMPC bubbles prepared in Isoton II or HEPES buffers and harvested after 3 or 20 min of flotation.

Significant differences in initial bubble size characteristics were observed between the two buffers. For the low DMPC concentration (10 mM), the mean radius of the bubbles prepared in HEPES was slightly, but significantly, larger than in Isoton II (5.9 vs $5.4 \mu\text{m}$) and the polydispersity was lower (± 0.2 vs $0.3 \mu\text{m}$). In HEPES, a minor population ($< 5\%$) of small bubbles with a mean radius of $\sim 1.5 \mu\text{m}$ was seen, which was not detected with Isoton II. For the high DMPC concentration (50 mM) and a short flotation time (3 min), the size distributions obtained in the two buffers were both bimodal (Figure 7b), with a dominant population centered at $\sim 5 \mu\text{m}$ in radius. When the flotation time was increased to 20 min (Figure 7c), the bubble size distributions became monomodal in both buffers, with a larger mean radius value in HEPES ($2.1 \pm 0.3 \mu\text{m}$) than in Isoton II ($1.6 \pm 0.4 \mu\text{m}$).

Table 1 summarizes the size characteristics of the PFH-stabilized microbubbles coated by DMPC and fractionated by gravity, as well as the size characteristics of PFB-stabilized microbubbles coated by DSPC and isolated by centrifugation.²⁷ The size characteristics of microbubbles obtained using CEHDA¹⁷ or a microfluidic process using a T-junction¹⁷ are also collected. The polydispersity indexes ($\% \text{ SD/mean diameter}$)¹⁷ are given to facilitate comparison.

(39) Corn  us, C.; Giulieri, F.; Krafft, M. P.; Riess, J. G. *Colloids Surf., A* **1993**, 70, 233–238.

(40) Kabalnov, A.; Klein, D.; Pelura, T.; Schutt, E.; Weers, J. *Ultrasound Med. Biol.* **1998**, 24, 739–749.

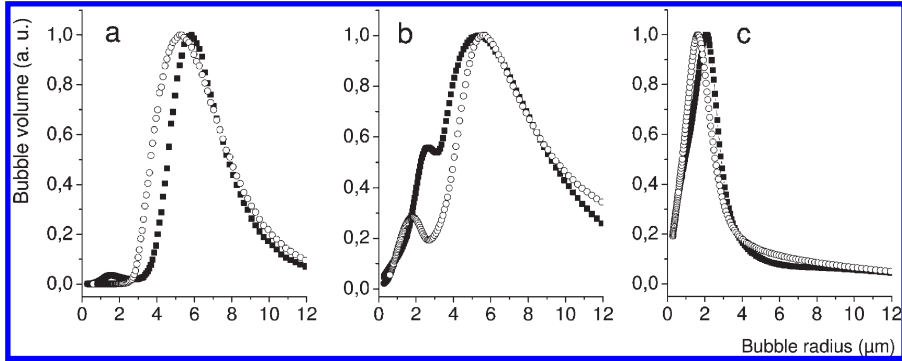


Figure 7. Initial size distributions of bubbles prepared in Isoton II (empty circles) or HEPES (full squares) from (a) a 10 mM-concentrated DMPC dispersion collected after 3 min of flotation or from a 50 mM-concentrated DMPC dispersion after (b) 3 or (c) 20 min of flotation.

Table 1. Size Characteristics of Phospholipid-Coated Microbubbles Prepared by Various Methods

preparation method	phospholipid/PFC gas/buffer	mean diameter (SD) (μm)		polydispersity index %
		population 1	population 2	
sonication				
crude (no fractionation)	L-α phosphatidylcholine/no PFC gas/distilled water	10.5 (18.5) ^{a,e}		176
separation by gravity	DMPC/PFH/Isoton II	10.8 (0.3) ^b	3.2 (0.4) ^b	2.8
	DMPC/PFH/HEPES	11.8 (0.2) ^c	4.2 (0.3) ^c	1.7
separation by centrifugation	DSPC/PFB/PBS	4.2 (0.1) ^d	1.8 (0.1) ^d	2.4
	CEHDA	6.6 (2.5) ^{a,e}		38
T-junction device	L-α phosphatidylcholine/no PFC gas/distilled water	30 (0.3) ^{a,e}		1

^a Ref 17. ^b Ref 26 and this work. ^c This work. ^d Ref 27. PBS, phosphate-buffered saline solution. ^e Only one population.

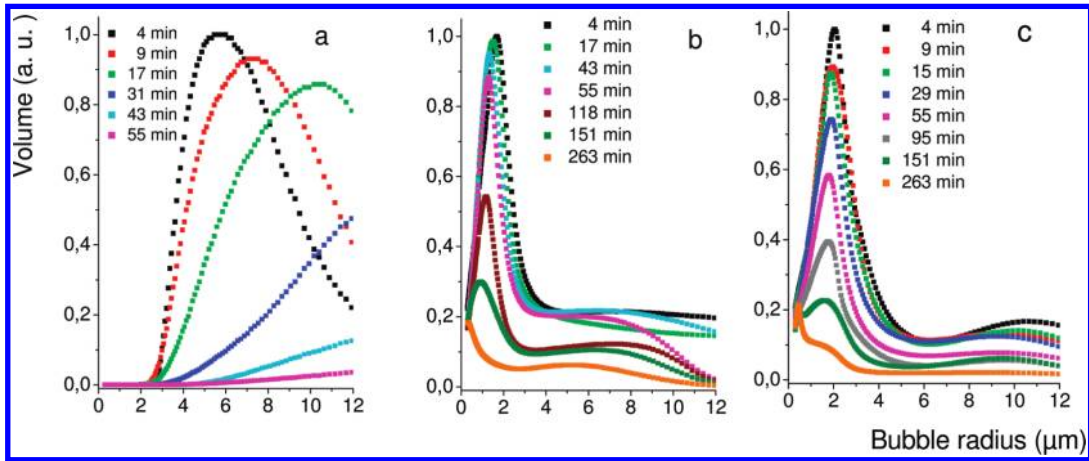


Figure 8. Time evolution at 25 °C of the size distributions of bubbles prepared from (a) a 10 mM DMPC dispersion in Isoton II separated after 3 min of flotation and a 50 mM DMPC dispersion in Isoton II (b) and in HEPES (c) buffers; bubbles in panels b and c were collected after 20 min of flotation.

It can be seen that sonication with fractionation (centrifugation or separation by gravity) is an efficient method for isolating suspensions of substantial amounts of narrowly dispersed populations of microbubbles having a size suitable for intravenous administration. The lowest diameter was obtained using sonication followed by centrifugation.²⁷ The T-junction device allows production of bubbles with the lowest polydispersity index.¹⁷ However, their mean diameter (30 μm) is large. CEDHA allows production of small bubbles with, however, a significantly larger polydispersity index than sonication with fractionation.

Microbubble Stability: Influence of Initial Bubble Size and Buffer. The samples investigated consisted of monomodal populations of large bubbles ($\sim 5.4 \pm 0.4 \mu\text{m}$ in radius in Isoton II and $\sim 5.9 \pm 0.2 \mu\text{m}$ in HEPES) prepared from 10 mM-concentrated dispersions allowed to float for 3 min and of monomodal

populations of small bubbles ($\sim 1.6 \pm 0.4 \mu\text{m}$ in Isoton II and $\sim 2.1 \pm 0.3 \mu\text{m}$ in HEPES) prepared from 50 mM dispersions allowed to float for 20 min. The internal phase consisted of PFH-saturated N_2 . The temporal evolutions of the radii distributions of the two types of bubbles are displayed on Figure 8.

It can be seen that upon aging, the population of large bubbles prepared in Isoton II was progressively shifted toward larger radii (Figure 8a). The same behavior was observed for similarly sized bubbles prepared in HEPES (data not shown). A strikingly different behavior was observed for the population of small bubbles. In Isoton II, the bubble radii were shifted toward smaller values; the initial radius was decreased by a factor of about two after about 2.5 h (Figure 8b). The behavior of small bubbles seems slightly differently in HEPES, their mean radius remaining essentially constant over time (Figure 8c). The difference noted

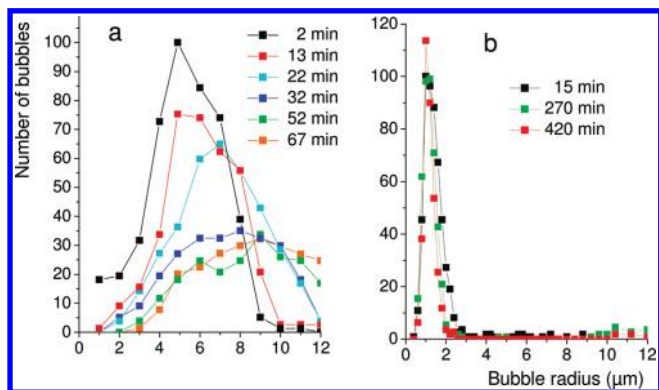


Figure 9. Time evolution at 25 °C of the size distributions of the large bubbles prepared in Isoton II (a) from a 10 mM DMPC dispersion and sampled after 3 min of flotation and (b) from a 50 mM DMPC dispersion sampled after 20 min, as assessed by optical microscopy.

between the two buffers investigated could be related to the nature of the counterions, which modify the dipolar interactions between the phospholipids' polar heads; salt bridges could also play a role. The above results were confirmed by optical microscopy observations (Figure 9), although the shift toward lower radii observed for the small bubbles was less precisely determined than by the acoustical method.

The variation of the bubble volume fraction determined acoustically was plotted as a function of time (Figure 10). It can be seen that the volume fraction decreased significantly more rapidly for the large bubbles than for the small bubbles, independently of the buffer. The half-life of the large bubbles ($\sim 5.4 \mu\text{m}$) prepared in Isoton II was $\sim 16 \pm 2$ min, as compared to $\sim 11 \pm 2$ min for the large bubbles ($\sim 5.9 \mu\text{m}$) prepared in HEPES. The small bubbles were observed to behave slightly differently depending on the buffer. In Isoton II, there was a delay (~ 20 min) during which the bubble volume fraction remained almost constant. In HEPES, on the other hand, the bubble volume fraction was found to decrease almost immediately. The half-lives of the small bubbles were $\sim 102 \pm 5$ and $\sim 88 \pm 5$ min in Isoton II and HEPES, respectively. Altogether, these results confirm and generalize the fact that small bubbles can last longer than larger ones in aqueous buffers.²⁶ A possible explanation could be that PFH, although it is not amphiphilic, actually acts as a cosurfactant with DMPC in the bubble shell, that is, once it is inserted in an organized layer of amphiphilic molecules. We have indeed reported that PFH strongly decreases the interfacial tension of DMPC at the air/aqueous phase interface and accelerates its adsorption at the interface.²⁶

The above data concur to suggest that the mechanisms of destabilization of small and large bubbles are different. While the larger bubbles consistently grow in size with time, which can be due to Ostwald ripening or coalescence, the small bubbles can retain their size or deflate only very slowly, likely by diffusion of the filling gas in the aqueous phase. It has previously been noted, in a study aiming at assessing the influence of the lipid shell characteristics on the destruction of the microbubbles by ultrasound,

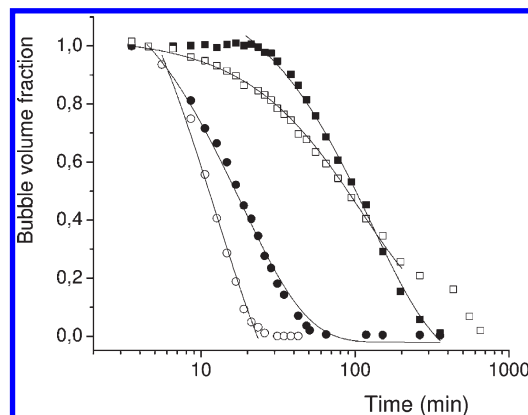


Figure 10. Time evolution at 25 °C of bubble volume for small bubbles prepared in Isoton II ($1.6 \mu\text{m}$, full squares) and in HEPES buffers ($2.1 \mu\text{m}$, empty squares) and of large bubbles prepared in Isoton II ($5.4 \mu\text{m}$, full circles) and in HEPES buffers ($\sim 5.9 \mu\text{m}$, empty circles) at 25 °C.

that the bubbles reached a critical size ($\sim 2 \mu\text{m}$) and were stable over many pulses at an intermediate acoustic pressure.⁴¹ However, the experiment was conducted over a very short time period, preventing determination of the half-life of the bubbles (which was not the object of the paper). Moreover, a possible effect of ultrasound power on the observed phenomena was not discarded. In our case, the low acoustic power attenuation measurements allow accurate determination and minimal perturbation of bubble sizes and size distributions over time.

Conclusions

Monomodal and narrowly distributed populations of bubbles of various mean sizes were sampled using the gravity field and were monitored over time using a multifrequency acoustical technique operating at a low acoustical power to avoid altering bubble stability. The production of differently sized microbubbles coated with DMPC and stabilized by PFH allowed determination of the effect of several composition parameters that influence the initial size and stability characteristics of these bubbles. We established that the temporal evolution of large and small bubbles follows different pathways. The radius of the large bubbles increases progressively over time, while that of the small bubbles decreases slightly or remains constant for several hours. This means that the mechanism of aging of large and small bubbles is different. A small but definite effect of the two buffers utilized as the aqueous phase was noted. These findings call for improved control of the size and dispersity of microbubbles destined for physicochemical and biomedical experimentation.

Acknowledgment. We thank the French Research Agency (ANR, Contract no. 06-BLAN-305-01) and the University of Strasbourg for financial support. S.R. acknowledges the ANR for a research fellowship.

(41) Borden, M. A.; Kruse, D. E.; Caskey, C. F.; Zhao, S.; Dayton, P. A.; Ferrara, K. *IEEE Trans. Ultrason. Ferroelectr., Freq. Contr.* **2005**, 52, 1992–2002.